Research Square

Preprints are preliminary reports that have not undergone peer review.
They should not be considered conclusive, used to inform clinical practice,
or referenced by the media as validated information.

# Human Breast Interstitium ("Hartveit's Labyrinth") and Its Relationship to Benign and Malignant Mammary Disease

**Stella Gordin**
NYU Grossman School of Medicine
**Luis A. Chiriboga**
NYU Grossman School of Medicine
**Brendan J. Belovarac**
NYU Grossman School of Medicine
**Farbod Darvishian**
NYU Grossman School of Medicine
**Ugur Ozerdem**
NYU Grossman School of Medicine
**Rebecca G. Wells**
University of Pennsylvania
**Sunil Badve**
Emory University School of Medicine
**Neil D. Theise**
neil.theise@nyulangone.org

NYU Grossman School of Medicine

**Article**

**Keywords:**

**Posted Date:** November 18th, 2026

**DOI:** https://doi.org/10.21203/rs.3.rs-11609611/v1

**License:** This work is licensed under a Creative Commons Attribution 4.0 International License.
Read Full License

**Additional Declarations:** No competing interests reported.

# Abstract

Flora Hartveit described a stromal “labyrinth” in the human female breast, but its organization and role in disease remain unclear. We examined interstitial spaces in archival specimens of normal breast, pseudoangiomatous stromal hyperplasia (PASH), and invasive lobular carcinoma using hyaluronic acid-binding protein histochemistry, single and multiplex immunohistochemistry, and collagen staining. In normal breast, hyaluronic acid-rich interstitial spaces spanned intercellular, pericapillary, and collagen-rich stromal compartments and continued into skin, vascular adventitia, perineurial connective tissue, and chest wall structures. In lobular carcinoma, tumor cells tracked through these spaces, sometimes approaching or entering lymphatics, without conspicuous stromal destruction. PASH clefts were hyaluronic acid-rich and lined by CD34-/vimentin-positive stromal cells with increased p16 and galectin-3 expression. These findings update Hartveit’s description, show continuity of the breast interstitium within and beyond the breast, and implicate it in stromal remodeling and local and lymphatic tumor spread.


# Introduction

The interstitium is a complex, body-wide network of fluid-filled spaces, rich in the glycosaminoglycan (GAG) hyaluronic acid (HA) with varied interrelationships with collagen and other extracellular matrix molecules depending on location (1–3). Interstitial spaces (IS) are found at three different scales, from the smallest, intercellular interstitium, through intermediate size pericapillary spaces across which tissue-vascular nutrient and waste exchanges take place, to the large scale “fascial interstitium” within the body-wide fascial system (1, 4–6). The smallest are generally less than 1.5 μm across and are found between select cell types (e.g., between keratinocytes, myocytes of all types, adipocytes) (6). The most well studied have been the intermediate size pericapillary IS often measuring 5–10 μm, though can be much larger for example in select tissues [1,5,6].

Interstitial spaces at the largest scale, sometimes referred to as the “fascial interstitium”, measures as much as 100 μm across and are demarcated by their supporting collagen bundles that often measure between approximately 10 and 20 μm [1,3,7,8]. These IS had long been largely unexplored because microscopy required dehydration, with tissue excision and in routine formalin-fixed, paraffin-embedded (FFPE) tissue preparation, leading to their artifactual collapse of the IS in final histologic sections (9).

These collagen-rich structures were comprehensively described by Franklin Mall, who called them a “reticular network” and believed them to be continuous across tissue and organ boundaries [10]. Mall’s conclusions have since been confirmed by modern decellularization techniques [11]. It has recently been suggested that these collagen-rich structures and the IS within them should be considered an organ system, namely, the “fascial system”, comprised of the fascia and the fascial interstitium [8].

Since interstitial spaces at all scales are rich in HA, its staining in histologic slides can map their distributions, thereby showing their continuity within tissues and organs and between them. Published examples using biotinylated hyaluronic acid binding protein (HABP) to stain for HA include skin and

superficial fascia, colon and mesentery, pulmonary system, and pancreas and duodenum and biliary tree (3, 12, 13). Also, the interstitial spaces within vascular adventitia (the connective tissue sheathes of all veins and arteries) and within perineurium (connective tissue sheathes of the peripheral nervous system) are continuous with the interstitial spaces of the tissues through which they pass (3, 12, 13). Since these perivascular and perineurial networks extend throughout the body, they provide spatial continuity of all interstitium throughout the body (1).

While recent descriptions of interstitial spaces in many organs were novel, in the human breast they were previously recognized by anatomic pathologist Flora Hartveit. They have been known eponymously as the “Hartveit labyrinth” or “Hartveit space” (14–17). Hartveit histologically identified stromal areas for electron microscopy sampling using toluidine blue (14–16). These ultrastructural studies, showed “attenuated cell processes lacking basement membrane, with specialized junctions and areas of close contact to connective tissue, that in part form channels, the lumina of which may be in direct connection with the stromal tissue spaces.”(14) Continuous with lymphatic stroma, they are a “pre-lymphatic space” and therefore, by definition, mammary interstitium. Three-dimensional reconstruction confirmed the continuity of these spaces, appearances of the lining cells, and continuity with lymphatics, as well as their distortions in pseudoangiomatous stromal hyperplasia (PASH) (18).

In this study we seek to update Hartveit’s characterization of these spaces using contemporary histochemical and immunohistochemical (IHC) staining techniques. We further explore interstitial alterations in benign and malignant diseases, namely PASH and invasive lobular carcinoma (ILC).

.

## METHODS

**Tissue samples and histochemical stains.**

Normal female breast tissues with overlying skin were sampled from breast reduction specimens for macromastia (n = 5). Tissues with pathology included excised breast tissues with PASH (n = 5) and mastectomy specimens containing invasive lobular carcinoma (n = 5).

# Histochemistry and Immunohistochemistry

Single marker and multiplex immunohistochemistry were performed on Ventana Medical Systems Discovery Ultra following best practices and using Ventana reagents except where noted [19,20]. All formalin fixed, paraffin-embedded samples were sectioned at four-microns and collected on plus slides (Epredia, Cat # TT-4041I-PS-8218-1) and stored at room temperature prior to use. Lyophilized biotinylated HABP was sourced from Sigma Aldrich (Catalog #385911, Lot# 4162326) and reconstituted according to manufacturer’s instructions. Antibody specifications are provided in supplemental table 1. Single marker IHC was performed according to the manufacturer’s instructions. Multiplexed antibody incubation, antigen retrieval and detection sequences were determined based on stand-alone protocol

requirements for each marker. Multiplex sequences were iteratively tested with crossover controls to eliminate primary-secondary antibody cross detection and verify that detection horseradish peroxidase (HRP) was quenched. Diluent only (no primary antibody) negative controls were included in the multiplex assay. All sample sets were run with tissue controls as positive, negative, and mIHC crossover controls. All slides were washed in distilled water, and lightly counterstained with hematoxylin (Epredia Cat# 7211) unless otherwise noted, followed by dehydration, clearing and mounting with permanent medium.

## Single marker Immunohistochemistry for p16 and Galectin-3

Mouse anti-human p16 INK4a was validated on cervical tissue. Mouse anti human galectin-3 was validated on colon carcinoma. Sections were deparaffinized using Discovery wash (Cat# 950– 510) for 4 minutes at 72°C. Antigen retrieval was performed in Ultra Cell Conditioner 1 (Cat# 950–224) for 48 minutes for p16 and for 36 minutes for Galectin-3 both at 95°C, followed by treatment with Inhibitor (Cat# 760–4840) for 4 minutes. Both P16 and Galectin 3 were ready-to use (RTU) and applied for 12 minutes and 16 minutes respectively at 37°C. P16 was detected with Optiview DAB detection (Cat# 760 – 700). Galectin-3 was detected with Ultraview DAB detection (Cat# 760 – 500).

## Multiplex Immunohistochemistry

# Multiplex immunohistochemistry for HABP-CD34-Podoplanin

These stains were performed as previously described [12,13]. Biotinylated HABP was used in a non-immune chromogenic assay. Murine anti-human CD34, and mouse anti-human Podoplanin were used. In brief, Sections were deparaffinized using Discovery wash (Cat# 950– 510) for 4 minutes at 72°C. Endogenous peroxidase was blocked with 3% hydrogen peroxide for 8 min at 37°C. HABP (Calbiochem Cat# 385911, Lot#4162326) was applied at 0.5 µg/ml (1:100 dilution) in tris-buffered saline with 1% bovine serum albumin (TBSA) and incubated for 12 h at room temperature. The biotinylated protein was then directly detected using HRP-conjugated streptavidin with DAB substrate (Ventana Cat# 760 – 124). Sections were then antigen-retrieved using Discovery Cell Conditioner 1(Cat# 950 – 500) for 20 min at 95°C. Inhibitor was reapplied. CD34 RTU was incubated for 20 min at 37°C followed by a goat anti-mouse HRP-conjugated Multimer (Ventana Cat# 760–4310) applied for 8 min at 37°C. CD34 was detected with purple chromogen (Ventana Cat# 760 – 229) for 8 min at 37°C. Sections were then denatured in Reaction Buffer (Ventana Cat# 950 – 300) for 32 min at 95°C. Inhibitor was reapplied. Podoplanin RTU was incubated for 2 hours at 37°C followed by a goat anti-mouse HRP- conjugated multimer (Ventana Cat# 760–4310) applied for 8 min at 37°C and detected using teal chromogen (Ventana Cat# 760 – 247) for 16 min at 37°C.

## Multiplex immunohistochemistry for Vimentin-p16 and Vimentin Galectin-3

These stains were performed using murine anti-human vimentin, and the same p16 and galectin-3 antibodies listed above. In both assays, Vimentin was applied first. Sections were deparaffinized using Discovery wash (Cat# 950– 510) for 4 minutes at 72°C. Antigen retrieval was performed in Ultra Cell Conditioner 1 (Cat# 950–224) for 24 minutes at 95°C. Endogenous peroxidase was blocked with 3% hydrogen peroxide for 8 min at 37°C. Vimentin was applied without dilution and incubated for 20 minutes at 37°C followed by a goat anti-mouse HRP-conjugated multimer (Ventana Cat# 760–4310) applied for 8 min at 37°C. Vimentin was detected with purple chromogen (Ventana Cat# 760 – 229) for 12 min at 37°C. Sections were then denatured in Reaction Buffer (Ventana Cat# 950 – 300) for 32 min at 95°C and inhibitor reapplied. Additional antigen retrieval was performed using Ultra Cell Conditioner 1. Vimentin-p16 was retrieved for 24 minutes at 91°C and 16 minutes at 91°C for Vimentin-Galectin-3. Vimentin-p16 was detected with goat anti-mouse HRP-conjugated multimer for 16 minutes at 37°C and Vimentin-Galectin-3 8 minutes at 37°C and both with Teal Chromogen for 12 minutes 37°C. Slides were washed dehydrated, cleared and mounted with permanent medium without counterstain.

# Co-Labeling Collagen and HA

HABP labeling was performed as described above. Upon completion, sections were extensively washed in distilled water and then were then stained with a modified Masson's Trichrome as follows. Sections were incubated in Phosphomolybdic-Phosphotungstic Acid for 13 minutes at room temperature and transferred directly into Analine Blue for 5 minutes. The sections were then rinsed in distilled water for 2 minutes and placed in 0.5% Acetic Acid in 70% Ethanol for 4 minutes. Sections were dehydrated in 3 changes of 95% and 3 changes of 100% ethanol followed by three changes of xylene and mounted with permanent media.

## Semi-quantification of p16 and Galectin-3

Each antigen was assessed for staining frequency within the examined PASH lesions and outside, in the adjacent, non-lesional breast parenchyma. Each was easily interpreted as dark brown staining. The results of the staining were graded semi-quantitatively according to prior procedures (21–23): 0, no positive cells; 1 +, rare positive cells that require careful searching at 20x magnification; 2+, scattered positive cells easily identified at 10x; 3+, clusters of positive cells apparent at 2x; and 4+, widespread positive staining apparent at 2x.

## Data Availability

Data sharing is not applicable to this article as no datasets were generated or analysed during the current study.

# RESULTS SECTION

**HA staining shows continuity between interstitial spaces throughout the breast stroma.**

Staining with HABP showed HA throughout the interstitial spaces of the normal breast tissue and demonstrated continuity across all stromal compartments by showing that what appear to be “empty” spaces with routine H&E stains are not empty but filled with HA (Fig. 1). The narrowest HA-filled interstitial spaces are between epidermal squamocytes and cells of the sebaceous glands (Fig. 1B). Continuity is evident from these spaces into the stroma of the papillary dermis, reticular dermis (Fig. 1B), and then into the stroma of the breast proper, including periductal (Fig. 1D), intralobular, and interlobular stroma (Fig. 1F).

The multiplex staining for HA, CD34 and D2-40 highlights the pericapillary interstitium and lymphatic networks. CD34 staining shows closed, round to oval loops of positive endothelial cells corresponding to arterioles, capillaries and venules. The intermediate scale HA filled spaces of the pericapillary interstitium are the tissue regions in which there is nutrient and waste exchange with the vascularized tissues (Fig. 1B,D,F,H). In the H&E stains, these regions – the papillary dermis, the periductal stroma, and the peri- and intralobular stroma appear pale and looser, but the HA staining of parallel shows the density and abundance of HA corresponding to the “empty”, pale spaces on the H&E. Podoplanin (D2-40) staining shows lymphatic endothelium of the superficial and deep lymphatics and those of the subareolar plexus (of Sappey) (some shown in Fig. 2A). At these sites, there is very occasionally seen the junction at which interstitial fluid flows from the HA-filled spaces into the open mouth of the lymphatic (Fig. 4D, E).

# Interstitial continuity beyond tissue boundaries of the breast

Throughout breast parenchyma there is interstitial continuity with the interstitium of perivascular adventitia (artery shown, Fig. 2A) and perineurium (Fig. 2B, pending). Continuity between breast parenchyma and the chest wall fascial planes and skeletal muscle is also confirmed (Fig. 2C, pending).

**Invasive lobular carcinoma cells move though interstitial spaces without significant tissue destruction and enter lymphatic channels.**

Invasive lobular carcinoma shows its typical perilobular invasive distribution (Fig. 3A), with extensive single-cell filing (Figs. 3B,C). The same pattern is highlighted in a different way, showing tumor cells (pale grey, round to oval) associated with surrounding, brown-stained HA moving between dense, collagen bundles highlighted with aniline blue. Inflammatory or stromal reactions are not seen in such areas, suggesting ease of tumor cell passage without the need for enzymatic stromal destruction. Lobular carcinoma approaches close to nerves through HA filled spaces (Fig. 3E). Occasionally,

malignant cells can be seen entering the open mouths of deep lymphatics at their juncture with stromal interstitium (Fig. 3F).

## Expression of keloid associated factors in PASH

All H&E sections of breast tissue with PASH showed typical thickened collagen bundles similar to keloid scars with spaces filled with HA (Fig. 4A-C). Cleft like spaces in PASH were widely lined by CD34 + interstitial lining cells (4+), but less so in non-lesional tissue (1 + to 2+) (Fig. 4C). Staining for p16 and Galectin-3 were similar, with 2 + to 3 + staining within PASH, but absent in adjacent non-lesional, normal appearing breast parenchyma (Fig. 4C). Duplex IHC for p16/vimentin confirmed widespread co-localization within PASH indicating p16 activation in stromal cells, as did PASH compared to normal breast tissue (Fig. 4D) and as did duplex IHC for galectin-3/vimentin (Fig. 4E). These patterns of staining are the same as those observed in dermal keloids.

# DISCUSSION

In normal and diseased female human breast tissues, staining for HA highlights all three scales of interstitium, intercellular, peri-capillary, and the largest within collagenized stroma, the “fascial” interstitium (Fig. 1). Intercellular interstitium is present in the squamous-lined tissues of the epidermis overlying the breast and of the most distal lactiferous ducts, and in sebaceous glands. Pericapillary interstitium is represented by the papillary dermis and the submucosae of the entire mammary duct network and lobules. The fascial interstitium of the breast comprises its collagenous stroma, which, like many locations in the body, such as the subcutis and mesentery (3, 4), is frequently intermixed with adipose tissue. The largest interstitial spaces were previously recognized by Hartveit as a “labyrinth” within the breast stroma. She described them as pre-lymphatic, i.e. the source for mammary lymph (14–16), and as a niche for mammary mast cells (17).

A probable function of the poroelastic properties of interstitium in normal, healthy breast tissues is to protect tissue integrity by helping it withstand mechanical stresses during distention (e.g. edema fluid accumulation, lactational changes) or compression (e.g. mechanical pressure, dehydration) (1). Interstitial changes in the lactating breast, particularly, may prove interesting for breast adaptations in the face of mechanical distortions during breast feeding (24). However, the mammary interstitium is not confined to the breast. It is also continuous with tissues beyond the breast through the interstitial spaces of the vascular adventitia, perineurium, and across the fascial boundary between the breast and the chest wall (Fig. 2). Thus, the breast interstitium is an integrated part of the body-wide interstitial network.

The normal breast interstitium, like other IS, is an in-tissue niche most prominently for three types of cells, including vimentin/CD34 positive fibroblastic interstitial lining cells demonstrated herein and previously described by Hartveit (3, 7, 14). Resident immunocytes and macrophages are also present, though non-macrophage mononuclear cells are rare in the absence of disease (1). However, when acute

or chronic inflammation occurs, immunocytes can enter the pericapillarly interstitium from the blood, and also traffic across the lymphatic/interstitial interfaces.

In regard to breast carcinoma, Hartveit's primary insight that the "labyrinth" was a potentially significant pathway for malignant invasion of stroma is confirmed (14, 25). The interstitium is an anatomic intermediate between a primary tumor and nearby blood vessels for vascular dissemination, along and into nerves (perineural invasion), into lymphatics for nodal spread, and by direct extension into chest wall across fascia into skeletal muscle or bone (Fig. 3). In the specific case of invasive lobular carcinoma, our current findings support the typical pattern of invasion known as "single-cell filing" reflects not only the poor cell cohesion attendant on E-cadherin loss, but also that the cells are frequently moving through the pre-existing, HA-filled interstitial spaces without tissue degradation (26). The solitary cells lining up within HA-filled spaces (Fig. 3A-D) mirrors the findings regarding breast cancer spread of Friedl et al, (27–30) This concept correlates with the increased invasiveness and metastasis of breast carcinoma when productive of hyaluronidases. (31, 32). It also may relate to lobular carcinoma cell expression of variants of CD44 – an HA receptor – that correlate with increased risk of lymphatic spread (33, 34).

The lack of a need for tumoral tissue degradation for malignancy to access the lymphatics through the interstitium is evidenced by how dyes or radioactive colloids injected into the breast for identification of sentinel lymph nodes passively follow the same routes (35). Other examples of foreign materials that could follow spread through the interstitium – and might therefore further support studies of interstitium in human tissues – include extruded or leaked silicone from implants (36).

There is also a possible relationship between the breast interstitium and early or late local recurrences of breast carcinoma. The mechanical force during primary tumor growth compresses the surrounding tissue stroma, causing a stress of increased interstitial fluid pressure within the tumor and significantly higher than normal interstitial fluid pressures in the peritumoral stroma (37, 38). These changes affect cancer cell migration through the interstitial channels by pushing the tumor cells out of the tumor and into adjacent "healthy" areas (27, 39). Local recurrences of breast cancer after wide excision or mastectomies with clear margins may be explained by long term habitation of tumor cells within the breast interstitium of the grossly and histologically uninvolved tissue (27, 40).

In terms of benign disease, a relationship between Hartveit's labyrinth and PASH has previously been suggested (18, 25). PASH sometimes called "interstitial hyperplasia", appears as an exaggerated version of normal breast interstitium with thickened, often hyalinized bundles of collagen within the mass with intervening slit-like spaces lined by fibroblastic spindle cells (18, 41). Like normal interstitial lining cells we confirm the slit-like spaces of PASH to be lined by cells positive for CD34 and vimentin, but negative for podoplanin and devoid of endothelial ultrastructural features (18, 40, 41). Our data further confirm the interstitium-like nature of PASH by showing that cleft-like spaces contain HA (Fig. 4A,B).

PASH lesions have strong histomorphologic similarities to dermal keloid and to stromal changes in systemic sclerosis (scleroderma). Both lesions have spindle cells showing marked upregulation of p16 by immunohistochemistry (42, 43). A known tumor suppressor protein, p16 expression is considered a

marker of cellular senescence and is increased (and often associated with diminished proliferative rates) in both keloidal and sclerodermal fibrosis (42, 43). We confirm similar p16 upregulation in vimentin positive stromal cells in PASH compared to normal background breast stroma in which it is largely absent (Fig. 4C).

Galectins are carbohydrate-binding proteins that are involved in diverse physiological functions, such as immunity and inflammation, cell migration, and autophagy and are linked to fibrosis, among other pathologies. Galectin-3 is normally expressed in dermal fibroblasts but increases in keloid and while fibroblast expression is diminished in early scleroderma, increased galectin-3 is seen with more severe and/or more advanced disease (44–47). Increased galactin-3 expression in keloidal and scleroderma are hypothesized to down-regulate intralesional inflammation, but increase fibroblast activation and collagen deposition perhaps through stimulation of TGF-beta (44–46). The same galectin-3 changes are seen in PASH (Fig. 4D).

These data suggest that PASH is a modified, reactive interstitium that has overlapping features with both keloidal and sclerodermal fibrosis. Therefore, PASH may either be abnormal cicatricial fibrosis following breast stromal injuries, or a local form of immune-mediated scarring, or both. However, the hormonal relationships seen in PASH are different than those seen in the other two diseases, however (48–51). So, while PASH pathogenesis and treatment may be similar in some ways to keloids and scleroderma, they may also differ in important ways.

Exosomes mediate cell–cell communication in the breast, locally and systemically. They are secreted by most cell types, and, given their presence in breast milk and production by breast cancer cells, are important in breast physiology (51–53). The breast interstitium, then, is necessarily the first tissue compartment into which exosomes are delivered from their cells of origin after which they can move through the interstitial labyrinth of the breast parenchyma, into the vascular supply across pericapillary interstitium, if not also beyond the breast through perivascular and perineural interstitia. Likewise, breast cancer cell exosome production and exosome-based chemotherapy delivery systems must involve interstitial pathways (54, 55).

The continuity we demonstrate between breast interstitium and those of the overlying skin and undergirding chest wall, must also be part of microbiome signaling pathways. Recent evidence suggests a physiologically active microbiome within the breast (56). Therefore, elements of microbial signaling might move through an entero-mammary pathway and across skin (areola) (57). The interstitium is a route linking all these structures together. thereby giving direct access for cutaneous microbiome to reach the deep interior of the breast.

We conclude that the interstitium of the human breast and its resident cell populations are the same as those described by Hartveit nearly thirty years ago, though in the intervening years they have remained a poorly defined area of anatomy. However, the interstitium’s distribution, continuity, composition, and cellular components are likely to be key to understanding normal breast physiology, stromal changes in response to injury and disease, and spread of malignancy, at least. This study focuses solely on the adult

human female breast. Structural and physiological differences are likely between from prepubescence, through adolescence, into adulthood, across monthly hormonal cycles and after menopause, and during lactation. Thus, the interstitium of the human female breast may prove a rich arena for scientific and clinical investigation.

## Declarations

# Competing interests

Authors SG, LAC, BJB, FD, UO, RGW, NDT declare no financial or non-financial competing interests. Author SB serves as Deputy Editor in Chief of this journal and had no role in the peer-review or decision to publish this manuscript.

# Author Contribution

SG: Planned and executed the study, performed specimen acquisition for normal and cancer specimens, image acquisition, data analysis, and figure preparation, co-wrote the manuscript LAC: Developed and performed all novel staining techniques, image acquisition and figure preparation, co-wrote the manuscript; BJB: performed specimen acquisition for PASH specimens, interpreted stained slides, data analysis, co-wrote manuscript; FD: Participated in study planning and oversight, data analysis, manuscript preparation; UO: participated in specimen acquisition, manuscript preparation; RGW: Conceptual planning of study, figure and manuscript preparation. SB: Conceptual planning of study, acquisition of study tissues, figure and manuscript preparation; NDT: Conceived, organized the study and its team, coordinated project development, image acquisition, data analysis, figure preparation, and co-wrote manuscript.

# Acknowledgements

The study received no funding.

## References

1. Wells, R. G. & Theise, N. D. Interstitial spaces: a basolateral source of structure and signals. *Annu. Rev. Cell Dev. Biol.* 42, 83–103 (2026). https://doi.org/10.1146/annurev-cellbio-111524-023144.
2. Khandekar, G. et al. Coordinated development of the mouse extrahepatic bile duct: implications for neonatal susceptibility to biliary injury. *J. Hepatol.* 72, 135–145 (2020). https://doi.org/10.1016/j.jhep.2019.08.036.
3. Cenaj, O. et al. Evidence for continuity of interstitial spaces across tissue and organ boundaries in humans. *Commun. Biol.* 4, 436 (2021). https://doi.org/10.1038/s42003-021-01962-0.

4. Swartz, M. A. & Fleury, M. E. Interstitial flow and its effects in soft tissues. *Annu. Rev. Biomed. Eng.* 9, 229–256 (2007). https://doi.org/10.1146/annurev.bioeng.9.060906.151850.
5. Wiig, H. & Swartz, M. A. Interstitial fluid and lymph formation and transport: physiological regulation and roles in inflammation and cancer. *Physiol. Rev.* 92, 1005–1060 (2012). https://doi.org/10.1152/physrev.00037.2011.
6. Benias, P. C. et al. Structure and distribution of an unrecognized interstitium in human tissues. *Sci. Rep.* 8, 4947 (2018). https://doi.org/10.1038/s41598-018-23062-6.
7. Theise, N. D., de Jong, I. E. M. & Wells, R. G. The interstitium of the mesentery: contents and inter-organ connections. In *The Mesentery and Inflammation* (eds Coffey, J. C. et al.) 37–55 (Springer, 2023). https://doi.org/10.1007/978-3-031-17774-3.
8. Stecco, C. et al. Towards a comprehensive definition of the human fascial system. *J. Anat.* 246, 1084–1098 (2025). https://doi.org/10.1111/joa.14212.
9. Comănescu, M., Arsene, D., Ardeleanu, C. & Bussolati, G. The mandate for a proper preservation in histopathological tissues. *Rom. J. Morphol. Embryol.* 53, 233–242 (2012).
10. Pirri, C., Wells, R. G., De Caro, R., Stecco, C. & Theise, N. D. What's old is new again: the anatomical studies of Franklin P. Mall and the fascial-interstitial spaces. *Clin. Anat.* 36, 887–895 (2023).
11. Kajbafzadeh, A. M. et al. A novel technique for simultaneous whole-body and multi-organ decellularization: umbilical artery catheterization as a perfusion-based method in a sheep foetus model. *Int. J. Exp. Pathol.* 96, 116–132 (2015). https://doi.org/10.1111/iep.12124.
12. Theise, N. D. et al. Evidence of interstitial continuity within and beyond the human pancreas. *Hum. Pathol.* 161, 105855 (2025). https://doi.org/10.1016/j.humpath.2025.105855.
13. Ordner, J. et al. Continuity of interstitial spaces within and outside the human lung. *J. Anat.* 247, 1059–1068 (2025). https://doi.org/10.1111/joa.14280.
14. Hartveit, E. Attenuated cells in breast stroma: the missing lymphatic system of the breast. *Histopathology* 16, 533–543 (1990). https://doi.org/10.1111/j.1365-2559.1990.tb01158.x.
15. Sandstad, E. & Hartveit, F. Stromal metachromasia: a marker for areas of incipient invasion in ductal carcinoma of the breast? *Histopathology* 11, 73–80 (1987). https://doi.org/10.1111/j.1365-2559.1987.tb02610.x.
16. Hartveit, F. Fat emboli in the lymphatic labyrinth in breast stroma. *Invasion Metastasis* 11, 227–232 (1991).
17. Hartveit, F. Mast cell association with collagen fibres in human breast stroma. *Eur. J. Morphol.* 31, 209–218 (1993).
18. Bolognesi, M. M. et al. Multiplex staining by sequential immunostaining and antibody removal on routine tissue sections. *J. Histochem. Cytochem.* 65, 431–444 (2017). https://doi.org/10.1369/0022155417719419.
19. Chiriboga, L., Callis, G. M., Wang, Y. & Chlipala, E. Guide for collecting and reporting metadata on protocol variables and parameters from slide-based histotechnology assays to enhance

reproducibility. *J. Histotechnol.* 45, 132–147 (2022). https://doi.org/10.1080/01478885.2022.2134022.

20. Theise, N. D., Conn, M. & Thung, S. N. Localization of cytomegalovirus antigens in liver allografts over time. *Hum. Pathol.* 24, 103–108 (1993). https://doi.org/10.1016/0046-8177(93)90069-S.
21. Park, Y. N. et al. Hepatic stellate cell activation in dysplastic nodules: evidence for an alternate hypothesis concerning human hepatocarcinogenesis. *Liver* 17, 271–274 (1997). https://doi.org/10.1111/j.1600-0676.1997.tb01031.x.
22. Levine, P. H., Delgado, Y., Theise, N. D. & West, A. B. Stellate-cell lipidosis in liver biopsy specimens: recognition and significance. *Am. J. Clin. Pathol.* 119, 254–258 (2003). https://doi.org/10.1309/6DKC-03C4-GAAE-N2DK.
23. Chen, P., Liao, Y. & Cai, J. Mammary adipocyte plasticity and epithelial crosstalk: roles in development, remodeling, and disease. *Rev. Endocr. Metab. Disord.* 27, 1023–1040 (2026). https://doi.org/10.1007/s11154-026-10065-2.
24. Vera-Sempere, F. J. & García Martínez, A. Laberinto de Hartveit e hiperplasia estromal seudoangiomatosa: una nueva ruta morfológica en la diseminación tumoral mamaria? *Med. Clin. (Barc.)* 121, 658–661 (2003).
25. McCart Reed, A. E., Kutasovic, J. R., Lakhani, S. R. & Simpson, P. T. Invasive lobular carcinoma of the breast: morphology, biomarkers and 'omics. *Breast Cancer Res.* 17, 12 (2015). https://doi.org/10.1186/s13058-015-0519-x.
26. Gritsenko, P. G., Ilina, O. & Friedl, P. Interstitial guidance of cancer invasion. *J. Pathol.* 226, 185–199 (2012). https://doi.org/10.1002/path.3031.
27. Wolf, K. et al. Collagen-based cell migration models in vitro and in vivo. *Semin. Cell Dev. Biol.* 20, 931–941 (2009). https://doi.org/10.1016/j.semcdb.2009.08.005.
28. Khalil, A. A. et al. Collective invasion in ductal and lobular breast cancer associates with distant metastasis. *Clin. Exp. Metastasis* 34, 421–429 (2017). https://doi.org/10.1007/s10585-017-9858-6.
29. Ilina, O. et al. Intravital microscopy of collective invasion plasticity in breast cancer. *Dis. Model. Mech.* 11, dmm034330 (2018). https://doi.org/10.1242/dmm.034330.
30. Fujisawa, S. et al. Clinicopathological significance of hyaluronan and hyaluronidase 2 (HYAL2) in breast cancer. *Pathol. Res. Pract.* 260, 155434 (2024). https://doi.org/10.1016/j.prp.2024.155434.
31. Wu, M. et al. A novel role of low molecular weight hyaluronan in breast cancer metastasis. *FASEB J.* 29, 1290–1298 (2015). https://doi.org/10.1096/fj.14-259978.
32. Dall, P. et al. Comparison of immunohistochemistry and RT-PCR for detection of CD44v-expression, a new prognostic factor in human breast cancer. *Int. J. Cancer* 60, 471–477 (1995). https://doi.org/10.1002/ijc.2910600408.
33. Berner, H. S. & Nesland, J. M. Expression of CD44 isoforms in infiltrating lobular carcinoma of the breast. *Breast Cancer Res. Treat.* 65, 23–29 (2001). https://doi.org/10.1023/A:1006417412046.

34. Proulx, S. T. & Detmar, M. Molecular mechanisms and imaging of lymphatic metastasis. *Exp. Cell Res.* 319, 1611–1617 (2013). https://doi.org/10.1016/j.yexcr.2013.03.009.
35. Pluvy, I. et al. Breast implant silicone exposure induces immunogenic response and autoimmune markers in human periprosthetic tissue. *Biomaterials* 317, 123025 (2025). https://doi.org/10.1016/j.biomaterials.2024.123025.
36. Agrawal, A. et al. Mechanical signatures in cancer metastasis. *npj Biol. Phys. Mech.* 2, 3 (2025). https://doi.org/10.1038/s44341-024-00007-x.
37. Rofstad, E. K., Galappathi, K. & Mathiesen, B. S. Tumor interstitial fluid pressure—a link between tumor hypoxia, microvascular density, and lymph node metastasis. *Neoplasia* 16, 586–594 (2014).
38. Salavati, H., Debbaut, C., Pullens, P. & Ceelen, W. Interstitial fluid pressure as an emerging biomarker in solid tumors. *Biochim. Biophys. Acta Rev. Cancer* 1877, 188792 (2022). https://doi.org/10.1016/j.bbcan.2022.188792.
39. Cackowski, F. C. & Korkaya, H. Breast cancer disseminated tumor cells: do they stay and fight or run and hide? *Cancer Res.* 84, 3319–3321 (2024). https://doi.org/10.1158/0008-5472.CAN-24-2408.
40. Bowman, E. et al. Pseudoangiomatous stromal hyperplasia (PASH) of the breast: a series of 24 patients. *Breast J.* 18, 242–247 (2012). https://doi.org/10.1111/j.1524-4741.2012.01230.x.
41. Koshy, R., Jain, P. V. & Jorns, J. M. Characterizing pseudoangiomatous stromal hyperplasia (PASH) of the breast. *Histopathology* 89, 174–180 (2026). https://doi.org/10.1111/his.70127.
42. Limandjaja, G. C. et al. Hypertrophic and keloid scars fail to progress from the CD34–/α-smooth muscle actin (α-SMA)+ immature scar phenotype and show gradient differences in α-SMA and p16 expression. *Br. J. Dermatol.* 182, 974–986 (2020). https://doi.org/10.1111/bjd.18219.
43. Tafuri, W. L. et al. Skin fibrosis associated with keloid, scleroderma and Jorge Lobo's disease (lacaziosis): an immuno-histochemical study. *Int. J. Exp. Pathol.* 103, 234–244 (2022). https://doi.org/10.1111/iep.12456.
44. Mora, G. F. & Rodríguez Zubieta, M. Galectin-1 and galectin-3 expression in lesional skin of patients with systemic sclerosis—association with disease severity. *J. Clin. Rheumatol.* 27, 317–323 (2021). https://doi.org/10.1097/RHU.0000000000001367.
45. Peiró, T. et al. Increased expression of galectin-3 in skin fibrosis: evidence from in vitro and in vivo studies. *Int. J. Mol. Sci.* 23, 15319 (2022). https://doi.org/10.3390/ijms232315319.
46. Arciniegas, E. et al. Galectin-1 and galectin-3 and their potential binding partners in the dermal thickening of keloid tissues. *Am. J. Dermatopathol.* 41, 193–204 (2019). https://doi.org/10.1097/DAD.0000000000001284.
47. Mackinnon, A. C. et al. Regulation of transforming growth factor-β1-driven lung fibrosis by galectin-3. *Am. J. Respir. Crit. Care Med.* 185, 537–546 (2012). https://doi.org/10.1164/rccm.201106-0965OC.
48. Peoples, C. et al. Gender differences in systemic sclerosis: relationship to clinical features, serologic status and outcomes. *J. Scleroderma Relat. Disord.* 1, 177–240 (2016). https://doi.org/10.5301/jsrd.5000209.

49. Rencic, A., Brinster, N. & Nousari, C. H. Keloid morphea and nodular scleroderma: two distinct clinical variants of scleroderma? *J. Cutan. Med. Surg.* 7, 20–24 (2003). https://doi.org/10.1007/s10227-002-1138-6.
50. Penmetsa, G. K. & Sapra, A. Morphea. In *StatPearls* (StatPearls Publishing, updated 2026).
51. Admyre, C. et al. Exosomes with immune modulatory features are present in human breast milk. *J. Immunol.* 179, 1969–1978 (2007). https://doi.org/10.4049/jimmunol.179.3.1969.
52. Melnik, B. C., Stremmel, W., Weiskirchen, R., John, S. M. & Schmitz, G. Exosome-derived microRNAs of human milk and their effects on infant health and development. *Biomolecules* 11, 851 (2021). https://doi.org/10.3390/biom11060851.
53. Tamkovich, S. et al. Exosomal microRNA: diagnostic potential and role in breast cancer dissemination. *Molecules* 30, 3858 (2025). https://doi.org/10.3390/molecules30193858.
54. Huang, S., Dong, M. & Chen, Q. Tumor-derived exosomes and their role in breast cancer metastasis. *Int. J. Mol. Sci.* 23, 13993 (2022). https://doi.org/10.3390/ijms232213993.
55. Weaver, J. W. et al. The application of exosomes in the treatment of triple-negative breast cancer. *Front. Mol. Biosci.* 9, 1022725 (2022). https://doi.org/10.3389/fmolb.2022.1022725.
56. Papakonstantinou, A. et al. The conundrum of breast cancer and microbiome—a comprehensive review of the current evidence. *Cancer Treat. Rev.* 111, 102470 (2022). https://doi.org/10.1016/j.ctrv.2022.102470.
57. Rodríguez, J. M. The origin of human milk bacteria: is there a bacterial entero-mammary pathway during late pregnancy and lactation? *Adv. Nutr.* 5, 779–784 (2014).

# Figures

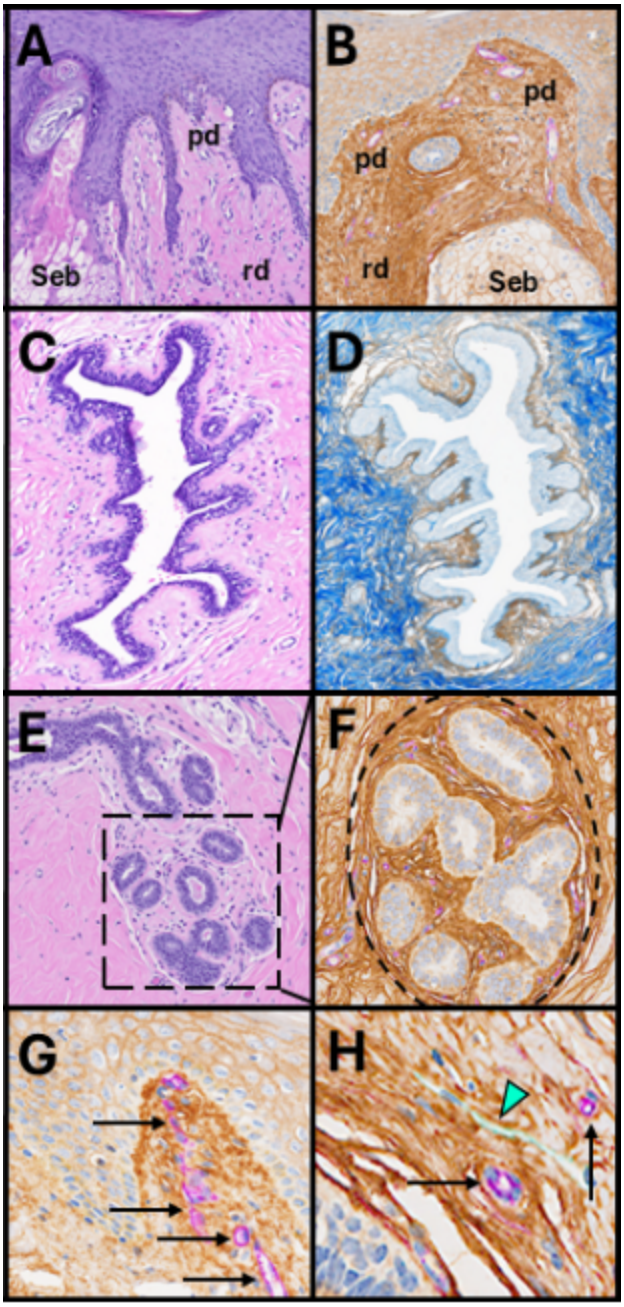



**Figure 1**

**Interstitium of normal human female breast.**

A. Skin of the nipple, showing epidermis at the top and papillary dermis (pd) and reticular dermis (rd) below. Adnexal sebaceous glands (seb) at lower left. (H&E, original magnification 2x.)

B. Staining for HA (brown) of parallel section to (A) showing intercellular interstitial spaces between epidermal keratinocytes and cells of the sebaceous glands (seb). (DAB, hematoxylin counterstain, original magnification 2x).

C. Mammary duct cross section with submucosal pale stoma surrounded by more densely staining stroma. (H&E, original magnification 10x.)

D. Staining for HA of parallel section to (C) with aniline blue counterstain of collagen. There is HA but thin, loosely aggregated collagen fibers in the submucosal region corresponding to the pericapillary interstitium. The much thicker, blue-stained collagen bundles of the “fascial” interstitium surround this region though HA still fills the interstitial spaces between them. (DAB, aniline blue counterstain, original magnification 10x).

E. Mammary duct and lobule with peri-lobular and intralobular stroma appearing more pale than denser stroma outside the duct/lobule unit. (H&E, original magnification 4x).

F. Staining for HA of parallel section to (E) showing abundant staining in the peri-lobular and intralobular stroma corresponding to the pericapillary interstitium (within dashed line), with less staining between thick collagen bundles in the larger scale “fascial” interstitium. Small, magenta, CD34-positive capillaries can be discerned in this region (HA/CD34/podoplanin triplex with DAB, hematoxylin counterstain. Original magnification 10x).

G. Higher magnification of the nipple epidermis and papillary dermis shows HA (brown) highlighting the intercellular interstitium of keratinocytes and the papillary dermis. Immunostain of CD34 (magenta) highlights capillaries (arrows) confirming this region as a peri-capillary interstitium. No podoplanin-positive lymphatics are not seen in this field (HA/CD34/podoplanin triplex with DAB, hematoxylin counterstain. Original magnification 100x).

H. Higher magnification of an edge of a duct (lower left) and the periductal stroma shows HA staining (brown) of the interstitium. Immunostain of CD34 (magenta) highlights capillaries (arrows) confirming this region as a peri-capillary interstitium. There is a podoplanin-positive lymphatic (green arrowhead). (HA/CD34/podoplanin triplex with DAB, hematoxylin counterstain. Original magnification 100x).

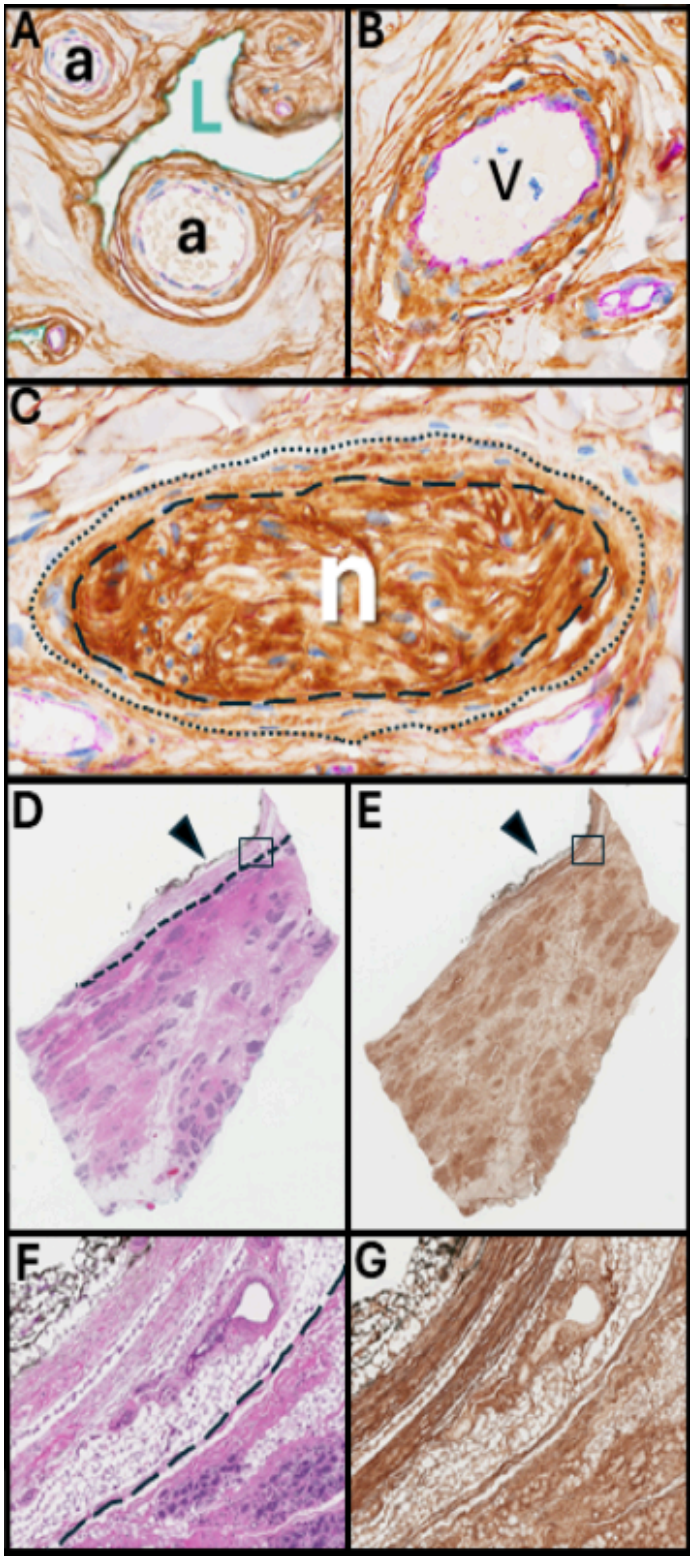



**Figure 2**

**Interstitial routes beyond the breast.**

A. Staining for HA (brown), shows the “empty” spaces, shows abundant HA between the pale grey collagen bundles of the breast stroma. In this cross section of a lymphovascular complex, two arteries (a) are lined by magenta, CD34-positive endothelial cells. A large lymphatic vessel is lined by podoplanin-

positive endothelium (teal). Magenta capillaries are located upper right. A smaller lymphovascular complex is at lower left with arteriole (magenta) and lymphangiole (teal). (HA/CD34/podoplanin triplex with DAB, hematoxylin counterstain. Original magnification 20x).

B. Staining for HA (brown), shows abundant HA in the adventitia surrounding a vein (v) with CD34-positive

endothelium. (HA/CD34/podoplanin triplex with DAB, hematoxylin counterstain. Original magnification 40x).

C. Abundant HA within a nerve (n, dashed line), within the perineurium (within the dotted line), and with interstitial spaces of the breast parenchyma beyond it. (HA/CD34/podoplanin triplex with DAB, hematoxylin counterstain. Original magnification 40x).

D. Whole mount of normal breast tissue with many dark blue mammary ducts and lobules (below and right of dashed line) and the adjoining chest wall fascia (above and left of the dashed line). There is black India ink applied to the deep margin of resection (black arrow). (H&E, Original magnification 1x).

E. The adjacent slide to (F) stained for HA showing continuity of HA staining across the breast-chest wall interface without interruption. (HA with DAB, hematoxylin counterstain. Original magnification 1x)

F. Higher magnification of (D, inset) the breast-chest wall interface on either side of the dashed line and black India ink highlighting the deep surgical resection margin (H&E, Original magnification 10x).

**G.** Higher magnification of (E, inset) the breast-chest wall interface shows continuity of HA filled interstitium across the interface. Black India ink highlights the deep surgical resection margin on the upper left (HA with DAB, hematoxylin counterstain. Original magnification 10x)

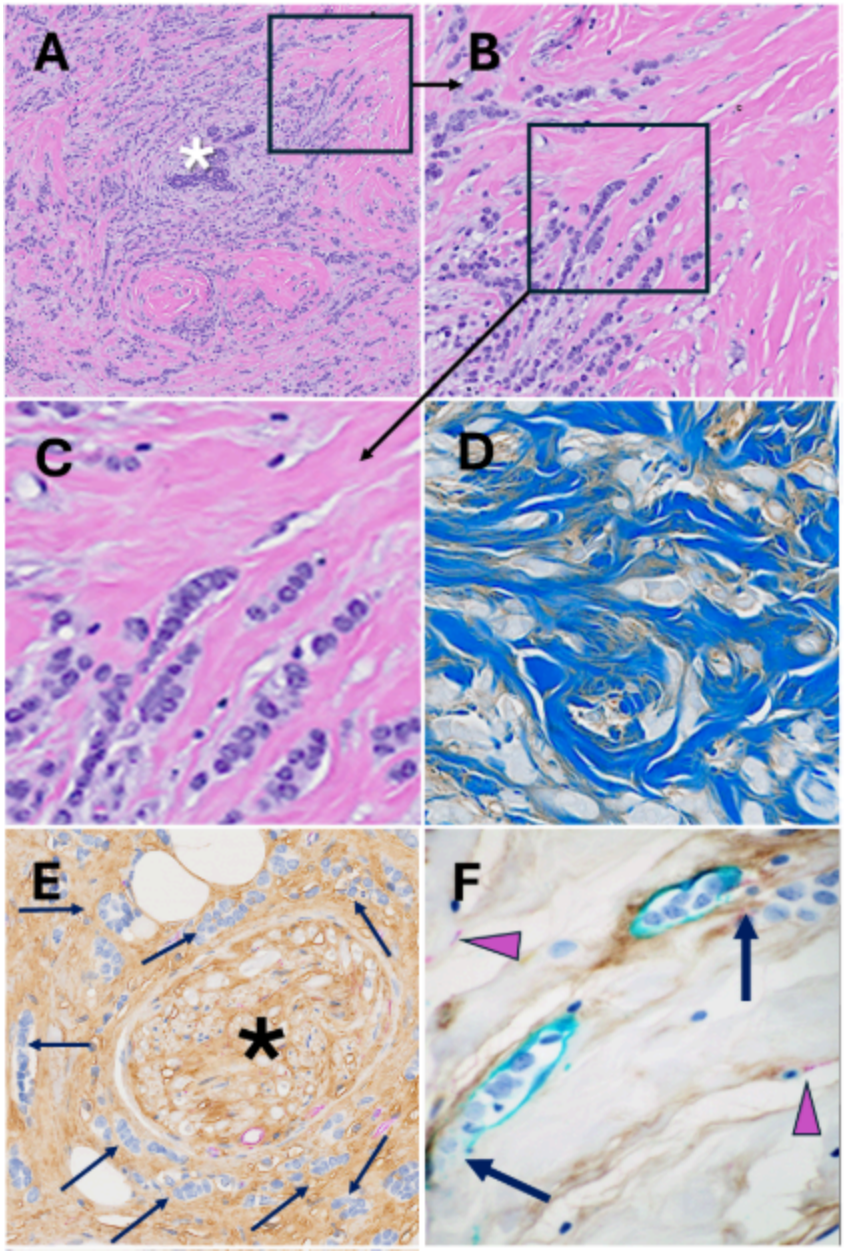



**Figure 3**

**Invasive lobular carcinoma and the interstitium**

A-C. Lobular carcinoma invading through breast parenchyma around a lobule (asterisk) with typical single-cell filing between collagen bundles, particularly at its advancing edge, where there is little inflammation or reactive changes in the stroma. (H&E, original magnifications: A. 4x, B. 10x, C. 20x.)

D. Single cell filing of lobular carcinoma (pale grey, round to oval) cells moving through HA (brown) filled interstitial spaces between original collagen bundles of the breast parenchyma (blue). There is little evidence of inflammation or stromal reactive changes. The malignant cells appear to have invaded through the pre-existing interstitial spaces rather than creating new paths by degrading the tissue by enzymatic digestion. (DAB, aniline blue, original magnification 40x.)

E. HA filling interstitial spaces around a nerve (asterisk) and within the nerve. Lobular carcinoma demonstrates single-cell filing in the interstitial spaces around the nerve and next to adjacent adipocytes (empty oval spaces). (HA/CD34/podoplanin triplex with DAB, hematoxylin counterstain. Original magnification 10x).

F. Lobular carcinoma cells (blue nuclei) moving through HA (brown) interstitium into the open stoma of lymphatics (arrows) highlighted by immunostaining of podoplanin (teal). Occasional CD34-positive (magenta) interstitial lining cells are seen (magenta arrowheads). (HA/CD34/podoplanin triplex with DAB, hematoxylin counterstain. Original magnification 20x.)

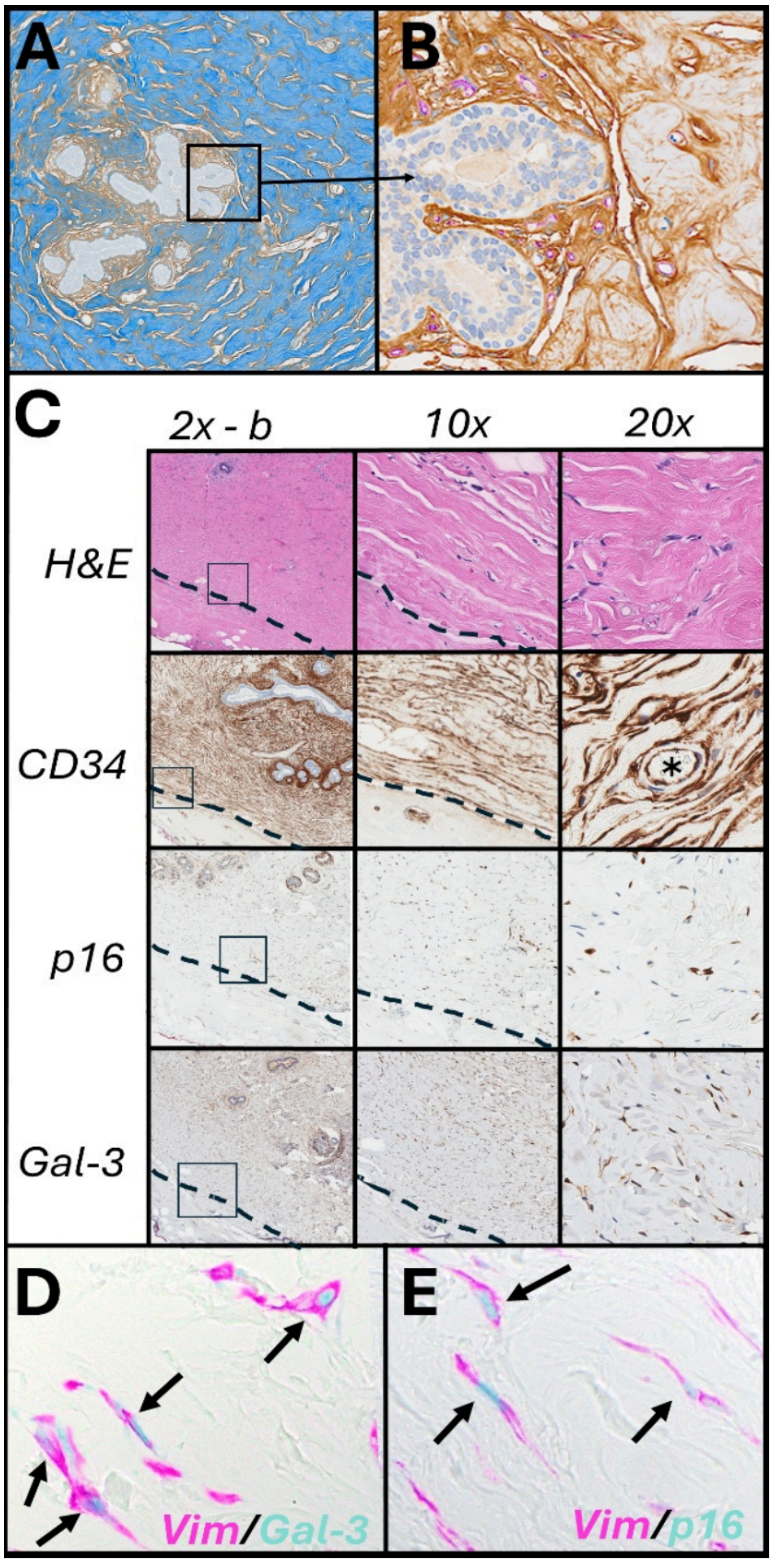



**Figure 4**

**Pseudoangiomatous hyperplasia (PASH) of the breast.**

A. Typical appearance of PASH with ducts and lobules surrounded by thickened collagen bundles with slit like spaces. These interstitial spaces are filled with HA (brown). (DAB, aniline blue. Original magnification 4x)

B. The stroma around the ducts show a normal appearing pericapillary interstitium (capillaries lined by magenta CD34-positive endothelial cells). HA filled spaces are seen between the pale grey, hyalinized PASH stroma (HA/CD34/podoplanin triplex with DAB, hematoxylin counterstain. Original magnification 20X.)

C. Low, medium and high power fields of the margin between normal breast parenhcyma (lower left) and PASH. H&A stain shows the typical keloid-like stroma of PASH with scattered lining cells within vascular-like clefts. These CD34-positive (brown) interstitial lining cells are more prominent and continuous within PASH than in the interstitium of the normal breast. Scattered lining cells are positive for p16 (brown) that are not seen in the adjacent normal tissue. Likewise, there are scattered galectin-3 lining cells within the PASH, though these are absent in the adjacent normal. (DAB, hematoxylin counterstain. Original magnifications: left, 2x; middle, 10x; right, 20x.)

D. Immunohistochemistry shows co-localization for vimentin (magenta) and galectin-3 (teal) confirming that interstitial lining cells of PASH up-regulate galectin-3 expression. Navy blue stain results in points of overlap between the two markers. (Original magnification 20x).

E. Immunohistochemistry shows co-localization for vimentin (magenta) and p-16 (teal) confirming that interstitial lining cells of PASH up-regulate p16 expression. Navy blue stain results in points of overlap between the two markers. (Original magnification 20x).

## Supplementary Files

This is a list of supplementary files associated with this preprint. Click to download.

- SupplementalTable1.docx